

# The analysis of tumor-infiltrating immune cell and ceRNA networks in laryngeal squamous cell carcinoma

Dan Li, MD<sup>a</sup> , Kaifeng Dong, MD<sup>a</sup>, Jing Su, MD<sup>a</sup>, Haitao Xue, MD<sup>a</sup>, Junhai Tian, MD<sup>a</sup>, Yongfeng Wu, MD<sup>a</sup>, Jingtian Wang, MD<sup>b,\*</sup>

## Abstract

**Background:** Laryngeal squamous cell carcinoma (LSCC) is one of the most common forms of head and neck cancers. However, few studies have focused on the correlation between competing endogenous RNA (ceRNAs) and immune cells in LSCC.

**Methods:** RNAseq expression of LSCC and adjacent tissues were downloaded from The Cancer Genome Atlas to establish a ceRNA network. The key gene in ceRNA was screened by the cox regression analysis to establish a prognostic risk assessment model. The CIBERSORT algorithm was then used to screen important tumor-infiltrating cells related to LSCC. Finally, co-expression analysis was applied to explore the relationship between key genes in the ceRNA network and tumor-infiltrating cells. The external datasets were used to validate critical biomarkers.

**Results:** We constructed a prognostic risk assessment model of key genes in the ceRNA network. As it turned out, Kaplan–Meier survival analysis showed significant differences in overall survival rates between high-risk and low-risk groups ( $P < .001$ ). The survival rate of the high-risk group was drastically lower than that of the low-risk group, and the AUC of 1 year, 3 years, and 5 years were all above 0.7. In addition, some immune infiltrating cells were also found to be related to LSCC. In the co-expression analysis, there is a negative correlation between plasma cells and TUBB3 ( $r = -0.33$ ,  $P = .0013$ ). External dataset validation also supports this result.

**Conclusion:** In this study, we found that some key genes (SLC35C1, CLDN23, HOXB7, STC2, TMEM158, TNFRSF4, TUBB3) and immune cells (plasma cells) may correspond to the prognosis of LSCC.

**Abbreviations:** ceRNA = competing endogenous RNA, DElncRNAs = differentially expressed lncRNAs, DEmRNAs = differentially expressed mRNAs, GEO = Gene Expression Omnibus, GO = Gene Ontology, HNSCC = head and neck squamous cell carcinoma, KEGG = Kyoto Encyclopedia of Genes and Genomes, LSCC = laryngeal squamous cell carcinoma, OS = overall survival, TCGA = The Cancer Genome Atlas.

**Keywords:** ceRNA networks, laryngeal squamous cell carcinoma, tumor-infiltrating immune cell

## 1. Introduction

Laryngeal cancer is a kind of malignant tumor of the head and neck, in which laryngeal squamous cell carcinoma (LSCC) is the most common, accounting for 96%–98%.<sup>[1]</sup> The incidence of LSCC is attributed to many factors such as smoking, excessive drinking, air pollution, sex hormone levels, and viral infections.<sup>[2]</sup> Recent years have witnessed the incidence of LSCC increase year by year with the acceleration of industrial processes and the aggravation of environmental pollution.<sup>[3]</sup> Currently, the main treatment methods involve surgery, chemotherapy, and radiotherapy. However, the complications from these treatments, as well as relapses and metastasis affecting the prognosis, can seriously interfere with a patient's normal life.<sup>[4]</sup> Therefore, early prevention, diagnosis, personalized

treatment, and the search for precise targeted therapeutic drugs are of great significance to increase the survival rate of patients. The treatment of LSCC requires the selection of appropriate treatment options according to the patient's clinical stages, metastasis ranges, tumor sizes, and ages. Surgical treatments are often applied for early LSCC, including total laryngectomy, partial laryngectomy, oral laser microsurgery, etc., quickly removing the lesions and effectively controlling the disease.<sup>[5]</sup> Unfortunately, the early symptoms of LSCC are not significant, and most patients are diagnosed in stage III or IV.<sup>[6]</sup> At this stage, the treatment effect of patients is not satisfactory to a certain extent.

Previous research presents a competing endogenous RNAs (ceRNA) hypothesis.<sup>[7]</sup> lncRNAs competitively bind to miRNAs, to regulate the expression level of mRNAs and involve in

The authors have no funding and conflicts of interest to declare.

The datasets presented in this study can be found in online repositories.

<sup>a</sup> Department of Otolaryngology, The First Hospital of Hebei Medical University, Hebei Province, China, <sup>b</sup> Otorhinolaryngology Surgery, The Fourth Hospital of Hebei Medical University, Hebei Province, China.

\* Correspondence: Jingtian Wang, MD, Otorhinolaryngology Surgery, The Fourth Hospital of Hebei Medical University, 12 Jiankang Road, Chang'an District, Shijiazhuang, Hebei Province 050011, China (e-mail: wangjingtian9985@sina.com).

Copyright © 2022 the Author(s). Published by Wolters Kluwer Health, Inc.

This is an open access article distributed under the Creative Commons Attribution License 4.0 (CCBY), which permits unrestricted use, distribution, and reproduction in any medium, provided the original work is properly cited.

How to cite this article: Li D, Dong K, Su J, Xue H, Tian J, Wu Y, Wang J. The analysis of tumor-infiltrating immune cell and ceRNA networks in laryngeal squamous cell carcinoma. *Medicine* 2022;101:31(e29555).

Received: 18 May 2021 / Received in final form: 29 March 2022 / Accepted: 21 April 2022

<http://dx.doi.org/10.1097/MD.00000000000029555>

the regulation of biological behaviors of tumor cells.<sup>[8–10]</sup> The ceRNA network plays a vital role in the development of various malignant tumors.<sup>[11–13]</sup> A large number of studies have shown that miRNA can guide RNA-induced silencing complex (RISC) to bind to target mRNA, leading to RNA degradation or translational inhibition.<sup>[14]</sup>

In recent years, tumor immune infiltrating cells have attracted widespread attention, especially in immunotherapy.<sup>[15]</sup> LSCC is rich in tumor immune infiltrating cells, and most patients respond positively to immunotherapy.<sup>[16]</sup> Some studies have shown that the different compositions and locations of tumor immune cells are closely related to the prognosis of LSCC.<sup>[17,18]</sup> However, in past studies, researchers used traditional methods, such as immunohistochemistry, to explore the composition of immune cells in malignant tumor tissues. The number of cells that these methods can detect is very limited.<sup>[19]</sup> With the development of various omics databases, some new methods for detecting immune cells based on machine learning have been born. For example, CIBERSORT, can estimate the abundance of 22 immune cell types from gene expression profiles.<sup>[20]</sup> Many studies use it to analyze the proportion of immune cells in cancer.<sup>[21,22]</sup>

Previous studies have separately reported the role of the ceRNA network and tumor immune cells in LSCC.<sup>[23,24]</sup> So far, there are only a few papers to comprehensively study the functions of ceRNAs and tumor immune cells in LSCC. Therefore, in this study, we hope to perform a co-expression analysis between ceRNAs and immune cells to identify potential immune-related biomarkers.

In this study, a ceRNA network for LSCC was established, which is determined by gene expression in the Cancer Genome Atlas (TCGA) database. The CIBERSORT was used to evaluate the proportion of immune cells in LSCC samples and quantify the cellular composition of the immune response. Afterward, genes in the ceRNA prognostic model and the key immune cells

that affect the prognosis were screened. Co-expression analysis of key genes and immune cells was carried out to explore the potential mechanisms affecting the prognosis of LSCC. As it turned out, these findings may provide new ideas for the prediction and treatment of LSCC. We show the experimental flowchart in Figure 1.

## 2. Materials and Methods

### 2.1. Data selection and analysis of differential gene expression

The RNAseq data of 123 patients with LSCC and normal samples were obtained from The Cancer Genome Atlas (TCGA) (Version October 21, 2020) (including 111 cases of cancer tissue and 12 cases of normal tissue adjacent to cancer) (<https://cancergenome.nih.gov/>).<sup>[25]</sup> The clinical data was downloaded by the Xena browser (<https://xenabrowser.net/>). Based on Ensembl annotation (<http://www.ensembl.org>), RNAseq data were divided into lncRNA and mRNA expression matrices.<sup>[26]</sup> Besides, the demographic information for each patient (age, gender, survival status, number of days of death, tumor stage, etc.) was downloaded. With R software and edgeR package, differentially expressed mRNAs (DEmRNAs) and differentially expressed lncRNAs (DELncRNAs) were obtained, and volcano maps and heat maps were drawn. The selection criteria for DEmRNAs and DELncRNAs is  $\log_{2}FC > 2.0$ ,  $P < .01$ .<sup>[27]</sup>

### 2.2. Construction of the ceRNA network

The mircode database (<http://www.mircode.org>) is used to identify the interactions between lncRNA and miRNA.<sup>[28]</sup> Then, miRNA target genes could be searched from miRDB databases.<sup>[29–31]</sup> After determining lncRNA-miRNA pairs and miRNA-mRNA pairs,

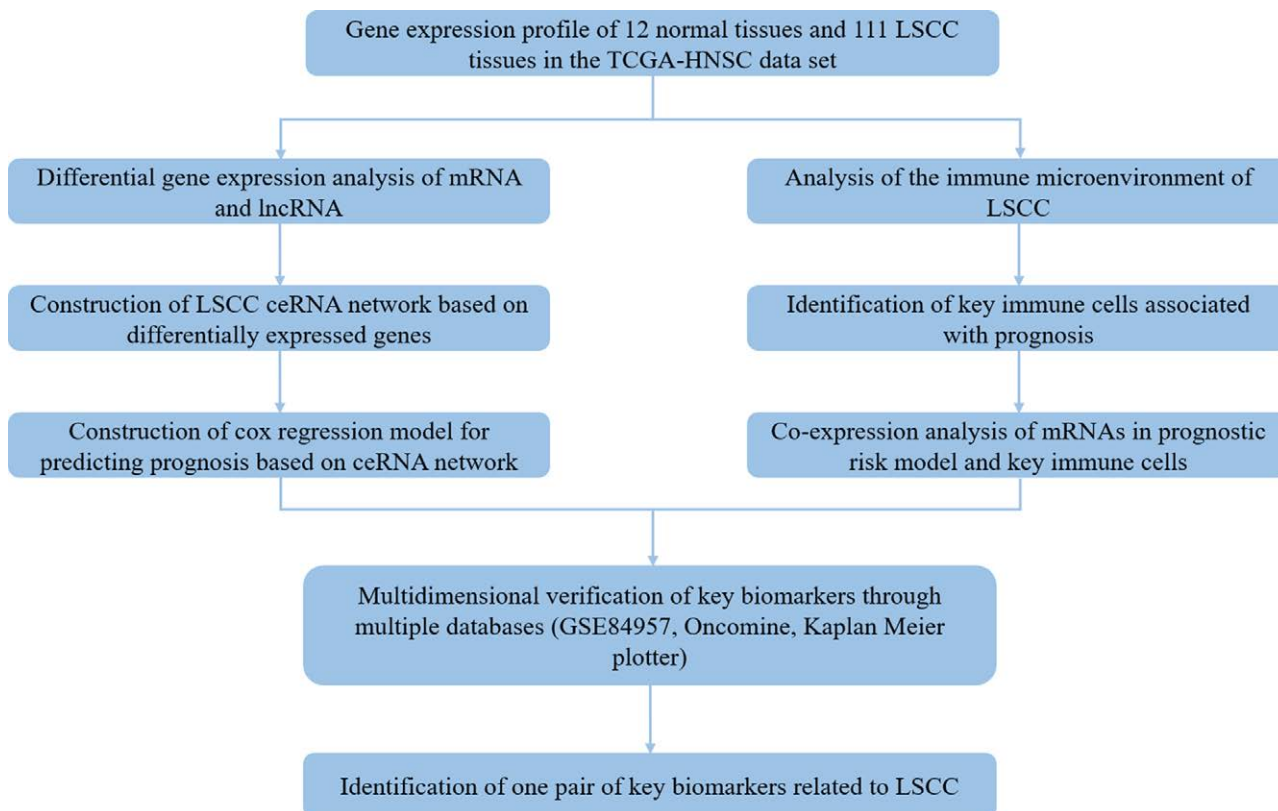


Figure 1. The experimental flowchart of this study.

**Table 1**  
Clinical information statistics of TCGA dataset.

Characteristic		TCGA dataset
Survival status	Alive	67
	Dead	50
Age	≤60	49
	>60	68
Sex	Female	20
	Male	97
Grade	G1	8
	G2	72
	G3	32
	G4	1
T	T1	7
	T2	14
	T3	26
	T4	55
N	N0	41
	N1	12
	N2	41
	N3	2
M	M0	41
	M1	9
Stage	I	2
	II	10
	III	14
	IV	74

we examined DEmRNAs and DELncRNA obtained from the edgeR package, respectively. Only lncRNA-miRNA and miRNA-mRNA pairs formed by differentially expressed RNA were screened. Eventually, we used Cytoscape v3.7 to construct the lncRNA-miRNA-mRNA network. The mRNA in the ceRNA network is the part that performs biological functions. Hence, the Gene Ontology (GO) and Kyoto Encyclopedia of Genes and Genomes (KEGG) enrichment analysis of these genes was performed to understand the biological functions of the network. The metasplice database was used for mRNA enrichment analysis (<https://metasplice.org/gp/index.html#/main/step1>).

### 2.3. Construction of prognostic risk model related to the ceRNA network

The expression data of each DEmRNA and DELncRNA in the ceRNA network was extracted, and we used the survival data

of each sample for single-variable COX regression analysis. The survival cox ph feature in R software was used and log-rank  $P < .05$  was chosen as the threshold for screening key genes that affect prognosis. Furthermore, the glmnet package in the R software is used to perform a set of cox regression analyses. After that, the prognostic risk assessment model of the ceRNA network is constructed with multivariable COX regression analysis. Based on the medium-risk score, we calculated the risk score for each sample separately and divided the patients into high-risk and low-risk groups, respectively. The Kaplan–Meier method was applied to analyze the difference in overall survival (OS) between 2 groups. Use the timeROC package of R software to draw ROC curves of 1, 3, and 5 years.

### 2.4. CIBERSORT estimation

The abundance of 22 different types of immune cells was estimated using CIBERSORT in R software (Version 4.0.2).<sup>[20]</sup> Wilcoxon rankings test identifies differences in immune infiltration between normal samples and patient samples. The result of  $P < .05$  indicates that the difference is statistically significant. In addition, corrplot and vioplot packages in R were also applied to visualize the results. The effects of immune cells on prognosis were analyzed by the Kaplan–Meier method.

### 2.5. Co-expression analysis of mRNAs in prognostic risk model and key immune cells

The corrplot package in R can be used for correlation analysis of 7 mRNAs and key immune cells. Under the Pearson correlation analysis, a co-expression heatmap was graphed to show the correlation between mRNAs and immune cells. The ggplot package in R was used to plot the correlation curves for mRNAs and immune cells that are highly correlated.

### 2.6. Multidimensional validation

The Gene Expression Omnibus (GEO) database is that of gene expression created and maintained by the National Center for Biotechnology Information. Moreover, it contains high-throughput gene expression data submitted by research institutions around the world.<sup>[32]</sup> The GSE84957 data set was used to confirm the expression of key genes in normal

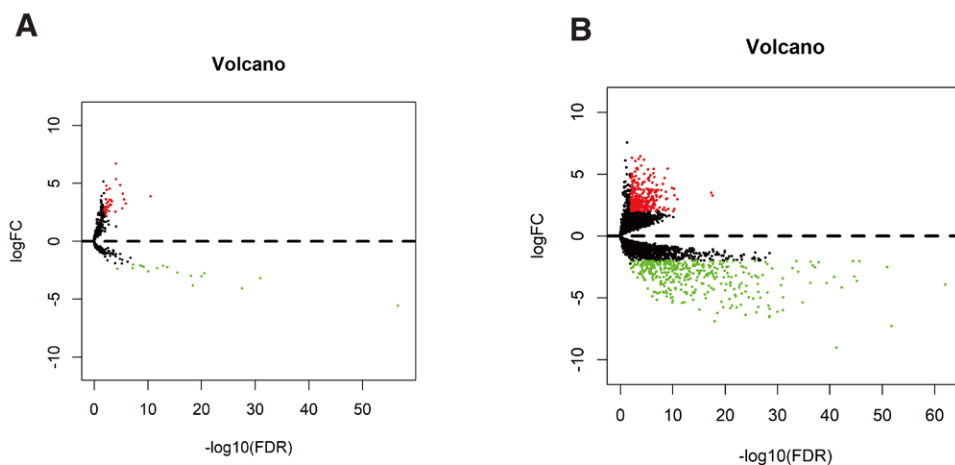


**Figure 2.** (A) Volcano map based on lncRNA expression values of 123 samples in TCGA database. Green represents low expression and red represents high expression. (B) Volcano map based on mRNA expression values of 123 samples in TCGA database. Green represents low expression and red represents high expression.

tissues and cancer tissues. All patients were provided written informed consent before their participation. The study was undertaken per the Institutional Ethics Committee of Beijing Tongren Hospital Affiliated with Capital Medical University and the ethical standards of the World Medical Association Declaration of Helsinki.<sup>[33]</sup> Kaplan Meier-plotter (<http://kmplot.com/analysis/index.php?p=service>) is a website for online survival analysis. Currently, the website has researched 54,675 genes and 18,674 cancer samples, involving breast cancer, lung cancer, gastric cancer, etc. Based on the Kaplan Meier-plotter website, it is used for survival analysis of critical mRNA. It can verify whether there is a significant difference in the survival time of patients at different expression levels.<sup>[34]</sup> In addition, oncoPrint was used to analyze the differential expression of key mRNAs in histological types of tumors and normal tissues (<https://www.oncoPrint.com/resource/login.html#>).<sup>[35]</sup>

### 3. Results

#### 3.1. Screening of differentially expressed genes and construction of the ceRNA network

There are 111 LSCC and 12 adjacent samples in the TCGA head and neck squamous cell carcinoma (HNSCC) dataset (Table 1). As shown in Figure 2, there are 662 DEMRNAs (289 mRNA upregulated, 373 mRNA downregulated) in LSCC samples; 57 DELncRNAs (39 upregulated, 18 downregulated) compared with adjacent tissues. Among these differentially expressed RNAs, we constructed a ceRNA network containing DELncRNAs and DEMRNAs, revealing the complex competition and connections between endogenous RNAs. We took advantage of Cytoscape 3.7.0 software to construct a ceRNA network with 58 nodes and 56 edges, including 3 lncRNAs, 15 miRNAs, and 40 mRNAs. The relationship between the different forms of RNA is illustrated in Figure 3A.

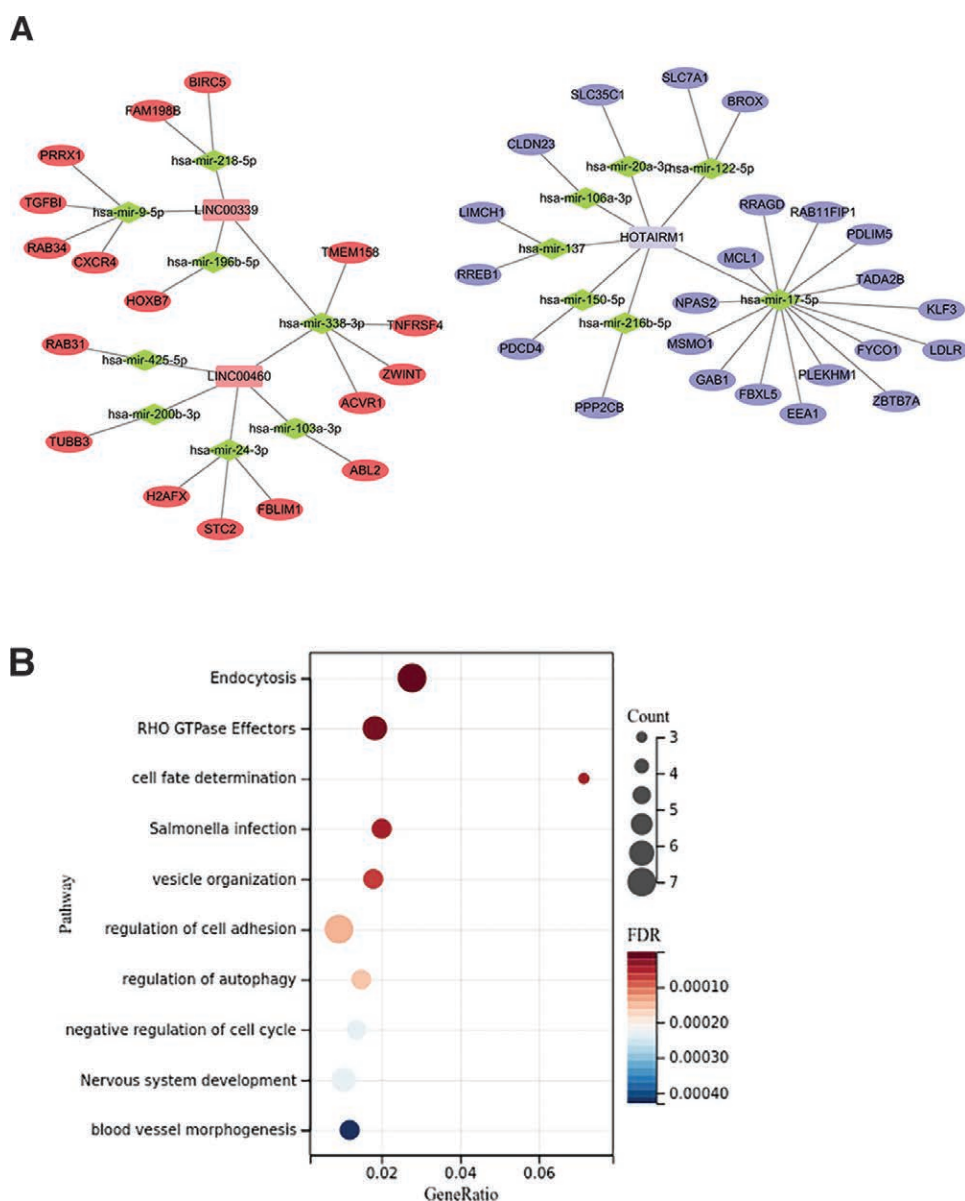


**Figure 3.** (A) Construction of the ceRNA network related to LSCC. Square nodes represent lncRNAs, where red is upregulated lncRNA and blue is downregulated lncRNA. Diamond-shaped nodes represent miRNAs. Oval nodes represent mRNAs, where red is upregulated mRNA and blue is downregulated mRNA. (B) Enrichment analysis of mRNAs in the ceRNA network.

Based on the metascape database, we carried out GO and KEGG enrichment analyses on mRNAs that performed biological functions in ceRNA (Figure 3B). The results indicate that these biological processes are mainly concentrated in endocytosis, RHO GTPase effectors, cell fate determination, salmonella infection, vesicle organization, regulation of cell adhesion, regulation of autophagy, negative regulation of cell cycle, nervous system development, blood vessel morphogenesis.

### 3.2. Analysis of prognostic risk model related to ceRNA network

First, we perform a univariate COX proportional hazard regression model on differentially expressed genes and survival data in the ceRNA networks. The results showed that 9

differentially expressed genes had a significant effect on the prognosis, all of which were mRNAs. We made use of the glmnet package in R to perform lasso cox regression analysis. In the first step, the change trajectory of each independent variable is displayed in Figure 4A. As the lambda increases, independent variable coefficients tend to gradually increase. We exploited a 10-fold crossover method to test the model, and then analyze the confidence interval for each lambda (Figure 4B). When lambda=0.013748, the model is optimal. The model at this point encompasses 8 mRNAs. Furthermore, we performed a multivariate cox regression analysis on the 8 mRNAs obtained in the previous step and retained the 7 mRNAs with the minimum AIC value (AIC = 359.51) as the final model (Figure 4C). The final 7-mRNA signature formula is as follows.

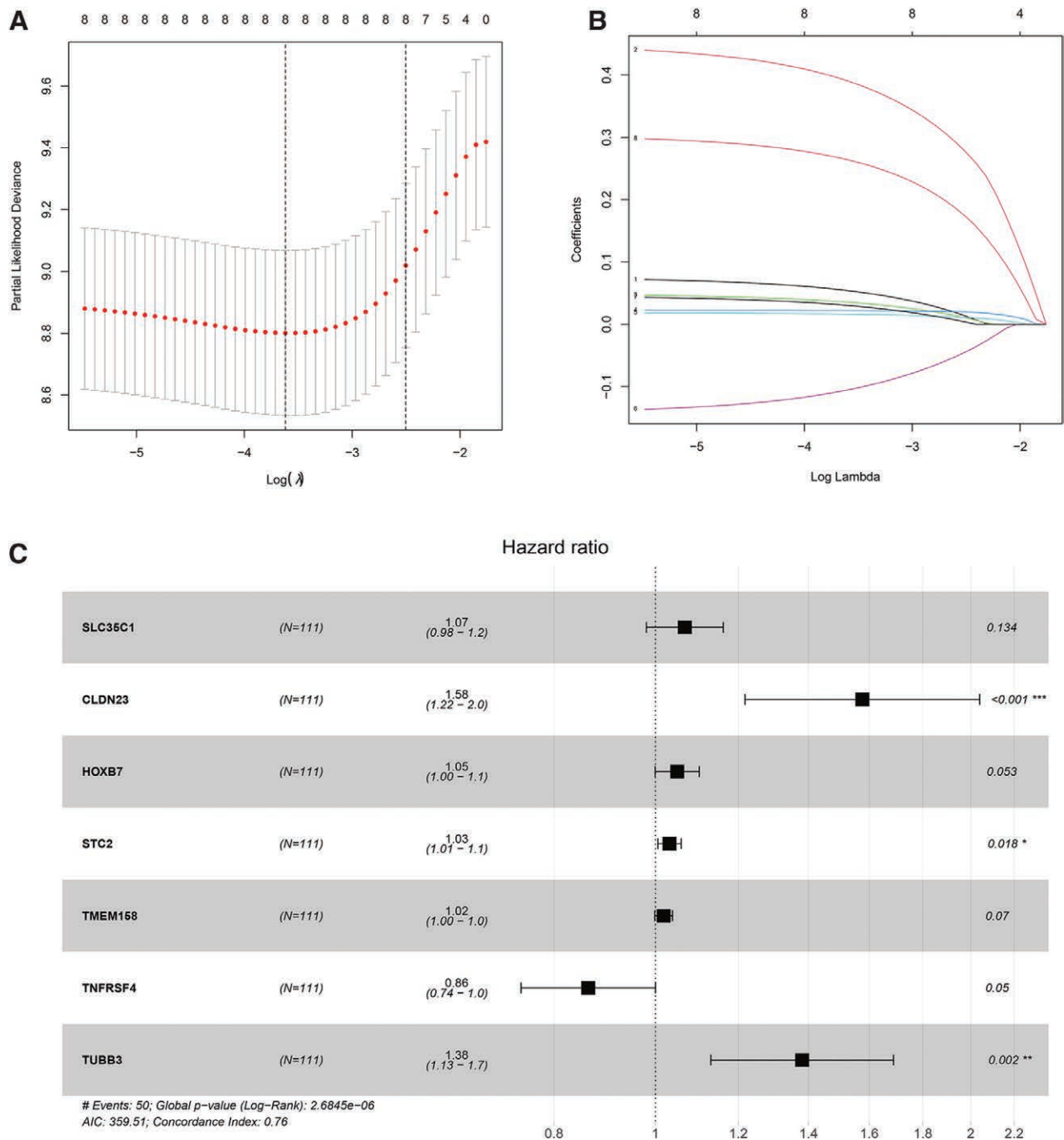


Figure 4. (A) LASSO model after 10-fold cross-validation. The 2 vertical dashed lines represent lambda.min and lambda.1se respectively. (B) Coefficient distribution of LASSO model. (C) Forest plot of the prognostic risk model of key genes in the ceRNA network. \* means that the difference is statistically significant.

$RiskScore = 0.065 * \exp SLC35C1 + 0.455 * \exp CLDN23 + 0.048 * \exp HOXB7 + 0.031 * \exp STC2 + 0.018 * \exp TMEM158 - 0.148 * \exp TNFRSF4 + 0.323 * \exp TUBB3$

To evaluate the prognostic effect of the model, the samples were divided into high-risk groups and low-risk groups. As is shown in Figures 5C–E, the distribution of risk scores based on the 7-mRNA signature model and their corresponding expression profiles in the TCGA-HNSCC dataset. Moreover, based on the analysis of the prediction accuracy rates of the model for 1, 3, and 5 years according to RiskScore, it can be seen that the model has a large area under the curve (AUC), and the AUC for 1, 3, and 5 years are all above 0.7 (Figures 5B). Kaplan–Meier survival analysis suggests the significant differences in the overall survival rate of the high-risk groups and the low-risk groups ( $P < .001$ ). The survival rate of patients in the high-risk group was significantly lower than that of the low-risk group (Figures 5A). These results indicate that RiskScore can effectively screen high-risk patients with poor clinical prognosis.

### 3.3. The composition of tumor-infiltrating immune cells of LSCC

The CIBERSORT algorithm was used to estimate the abundance of 22 immune cells. The distribution of tumor-infiltrating immune cells in normal and patient samples is shown in Figure 6A. It shows immune cell types and relative percent in LSCC tissues. Figure 6B is the heatmap of tumor-infiltrating cells in LSCC tissues and control group tissues. The correlation analysis of immune cells showed that Monocytes, B cells naïve and plasma cells were positively correlated. T cells CD8 and T cells CD4 memory activated are positively correlated. Monocytes, B cells naïve, plasma cells, and T cells CD8 are all negatively correlated with Macrophages M0. Furthermore, Dendritic cells activated and Mast cells activated are negatively correlated with Macrophages M1 (Fig. 7A). In the violin chart (Fig. 7B), the

Wilcoxon rank-sum test showed that B cells, Monocytes, and Macrophages M0 in normal tissues and tumor tissues are different. B cells and monocytes are present at lower concentrations in tumors while M0 macrophages are more abundant. The survival analysis showed that Dendritic cells resting ( $P = .021$ ) and plasma cells ( $P = .002$ ) may be correlated with the prognosis of LSCC patients (Fig. 8).

### 3.4. Co-expression analysis of mRNAs in prognostic risk model and key immune cells

To explore the correlation between key RNAs and prognosis-related immune cells, we performed a Pearson correlation analysis (Fig. 9). The results showed significant correlations between SLC35C1 and CLDN23 ( $R = 0.36, P < .001$ ), STC2 and TMEM158 ( $R = 0.53, P < .001$ ), and TUBB3 and plasma cells ( $R = -0.33, P = .0013$ ). Further co-expression analysis also revealed a significant positive correlation between SLC35C1 and CLDN23, STC2 and TMEM158, and a significant negative correlation between TUBB3 and plasma cells.

### 3.5. Multidimensional validation

The GSE84957 microarray in the GEO database contains 9 primary LSCC tissues and 9 corresponding adjacent non-tumor tissues. For that matter, it was used to verify the expression levels of 7 key genes. Admittedly, compared with normal tissues, SLC35C1, CLDN23 and TNFRSF4 were significantly downregulated in LSCC tissues ( $P < .05$ ), HOXB7, STC2, TMEM158, and TUBB3 were significantly upregulated in LSCC tissues ( $P < .05$ , Figure 10A). In the TCGA database, compared with normal tissues, SLC35C1 and CLDN23 were significantly downregulated in LSCC tissues ( $P < .05$ ), and HOXB7, STC2, TMEM158, TNFRSF4, and TUBB3 were

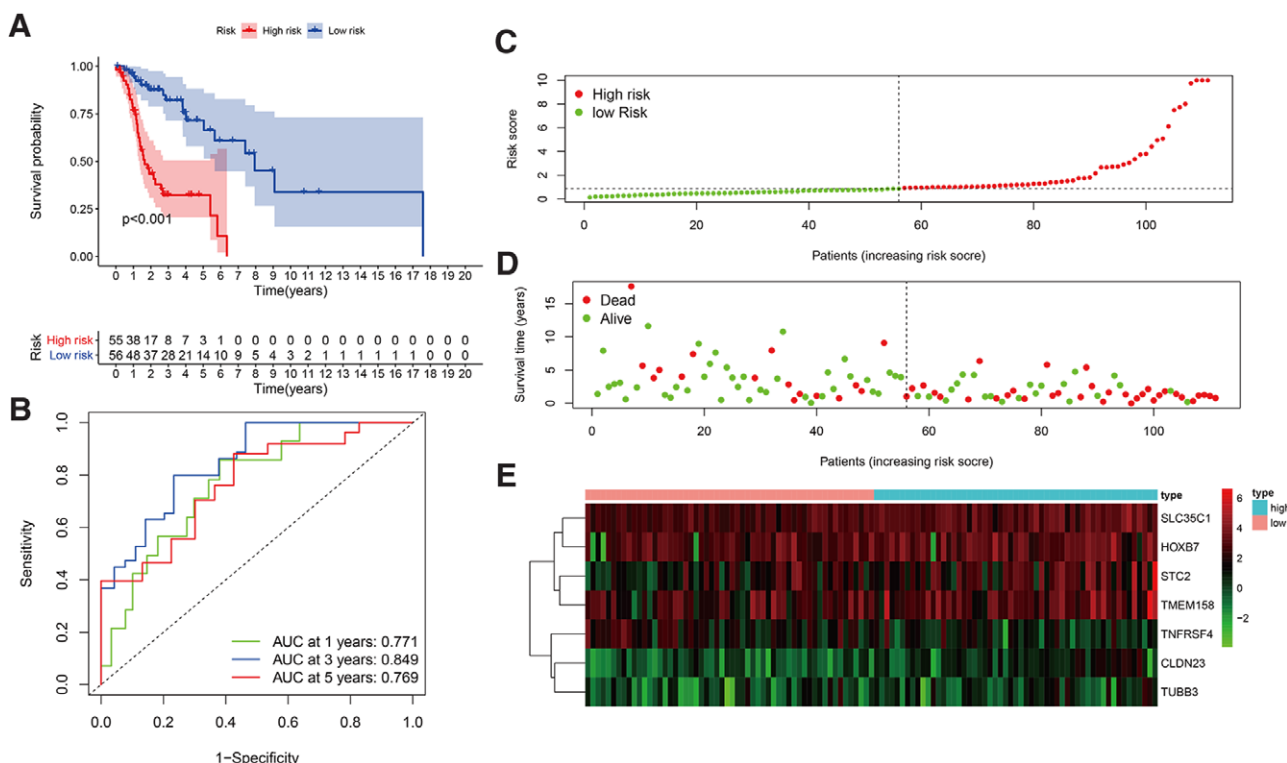


**Figure 5.** (A) The overall survival curve of high-risk and low-risk patients based on Kaplan–Meier analysis. (B) 1-year, 3-year, and 5-year ROC curves based on prognostic model. (C) Distribution of risk scores for patients with LSCC. (D) Risk score and survival status of patients with LSCC. (E) Heatmaps of key mRNA expression values in samples of the high-risk and low-risk groups.

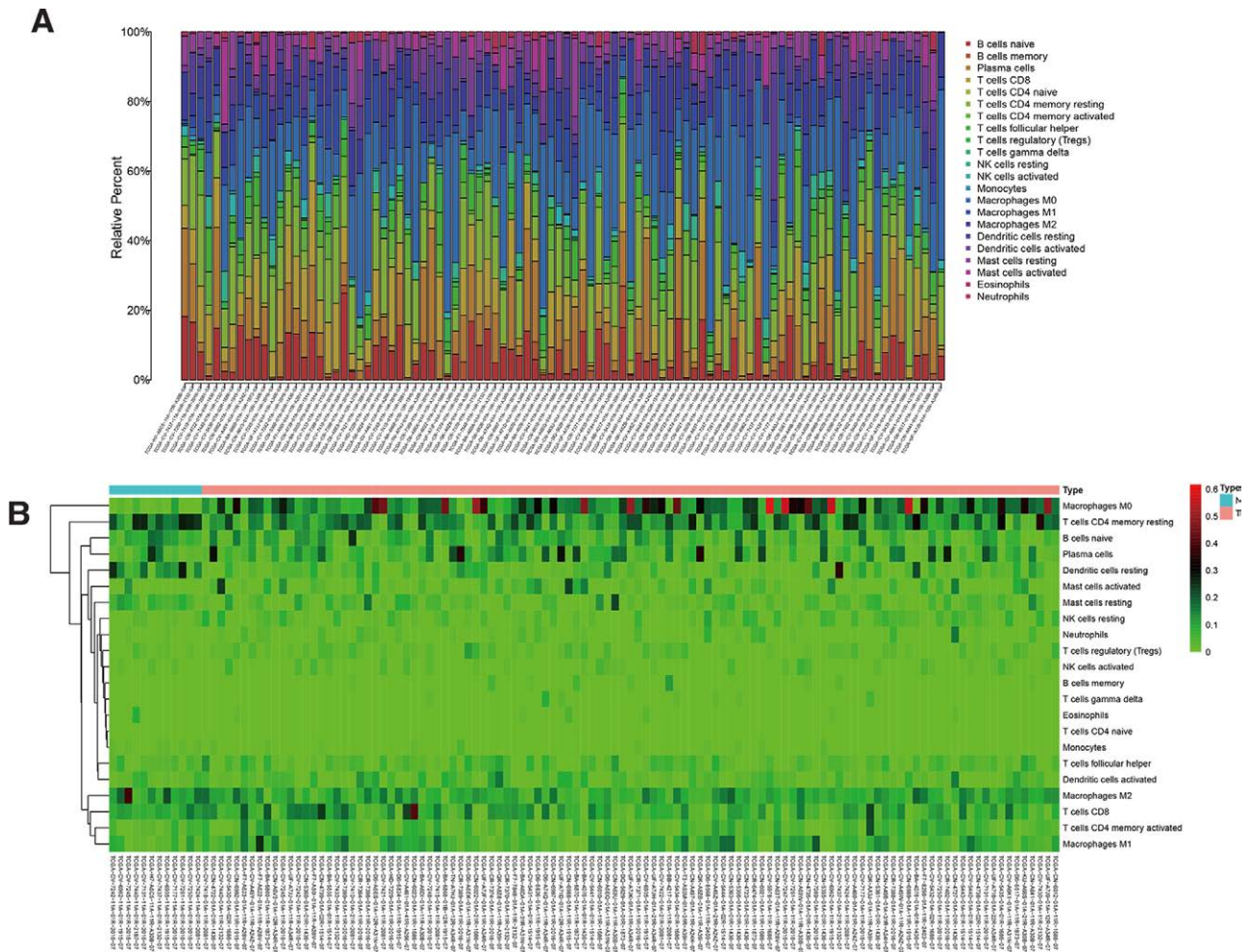


**Figure 6.** (A) Histogram of immune cell infiltration in TCGA samples. The abscissa represents the sample name, and the ordinate represents the percentage of immune cells. Different colored bars represent different immune cells. (B) Heatmap of immune cell infiltration in each sample. The abscissa is the sample name, and the ordinate is 22 immune cells. The shade of color represents the relative expression of immune cells.

significantly upregulated in LSCC tissues ( $P < .05$ , Figure 10B). The expression level of TNFRSF4 in GEO and TCGA databases is inconsistent. According to previous studies, the expression level of TNFRSF4 is controversial. Both high and low expressions of TNFRSF4 have been reported in tumor tissues.<sup>[36,37]</sup>

We used the oncomine database to analyze the expression levels of key genes for different types of cancer (oncomine parameter selection  $P$  value  $< .01$ ,  $\log_{2}FC > 1.5$ , generank selection top 10%). As shown in Figure 10C, red boxes indicate high expression and blue boxes indicate low expression. The numbers in the table represent the number of studies included in the oncomine database. The Kaplan–Meier method was further used to analyze critical mRNAs to assess their impact on overall survival (Figure 10D). Among them, the high expressions of SLC35C1, CLDN23, HOXB7, STC2, TMEM158, and TUBB3 are all related to patients with poor prognostic ( $P < .05$ ), and the high expression of TNFRSF4 is related to the better one ( $P < .05$ ). In the calculation results of TCGA and GEO, HOXB7, STC2, TMEM158, and TUBB3 genes are all highly expressed in patients. This is consistent with their high expression and poor prognosis. TNFRSF4 is low expression in patients, which is consistent with high expression and better prognosis in patients.

#### 4. Discussion

After the differentially expressed ceRNA network between LSCC and adjacent tissues and the key immune cells in the

tumor microenvironment has been identified, we constructed a prognostic prediction model based on the selected ceRNA network and immune cells. In this regard, SLC35C1, CLDN23, HOXB7, STC2, TMEM158, TNFRSF4, and TUBB3 in the model can effectively predict the prognosis. SLC35C1 and CLDN23 are downregulated in most cancers.<sup>[38–41]</sup> HOXB7, STC2, TMEM158, and TUBB3 are upregulated in most cancers (Figure 10C). For example, HOXB7 is highly expressed in breast cancer, ovarian cancer, and melanoma samples.<sup>[42–45]</sup> STC2 is highly expressed in rectal cancer and colon cancer.<sup>[46,47]</sup> TMEM158 is upregulated in laryngeal cancer, glioblastoma, and colorectal cancer.<sup>[48–50]</sup> TUBB3 is upregulated in gastric cancer, gallbladder cancer, and ovarian cancer.<sup>[51–53]</sup> STC2 is the encoding gene for stanniocalcin-2. One study investigated the expression of STC2 in 70 esophageal cancer cell lines. The expression of STC2 in cancer tissues was higher than in the corresponding normal tissues ( $P < .001$ ). Additionally, STC2 expression was significantly associated with lymph node metastasis, lymphatic invasion, and long-range metastasis ( $P = .005$ ,  $.007$ , and  $.038$ , respectively). Obviously, the 5-year survival rate of patients with high STC2 expression was lower than those with low STC2 expression rates ( $P = .016$ ). In vitro experiments showed that the proliferation rate of STC2 transfected cells was significantly higher than that of control cells ( $P < .001$ ). STC2 transfected cells were also more aggressive than the control cells ( $P < .001$ ).<sup>[35]</sup> TMEM158 is a gene that encodes transmembrane protein 158. Its upregulation promotes

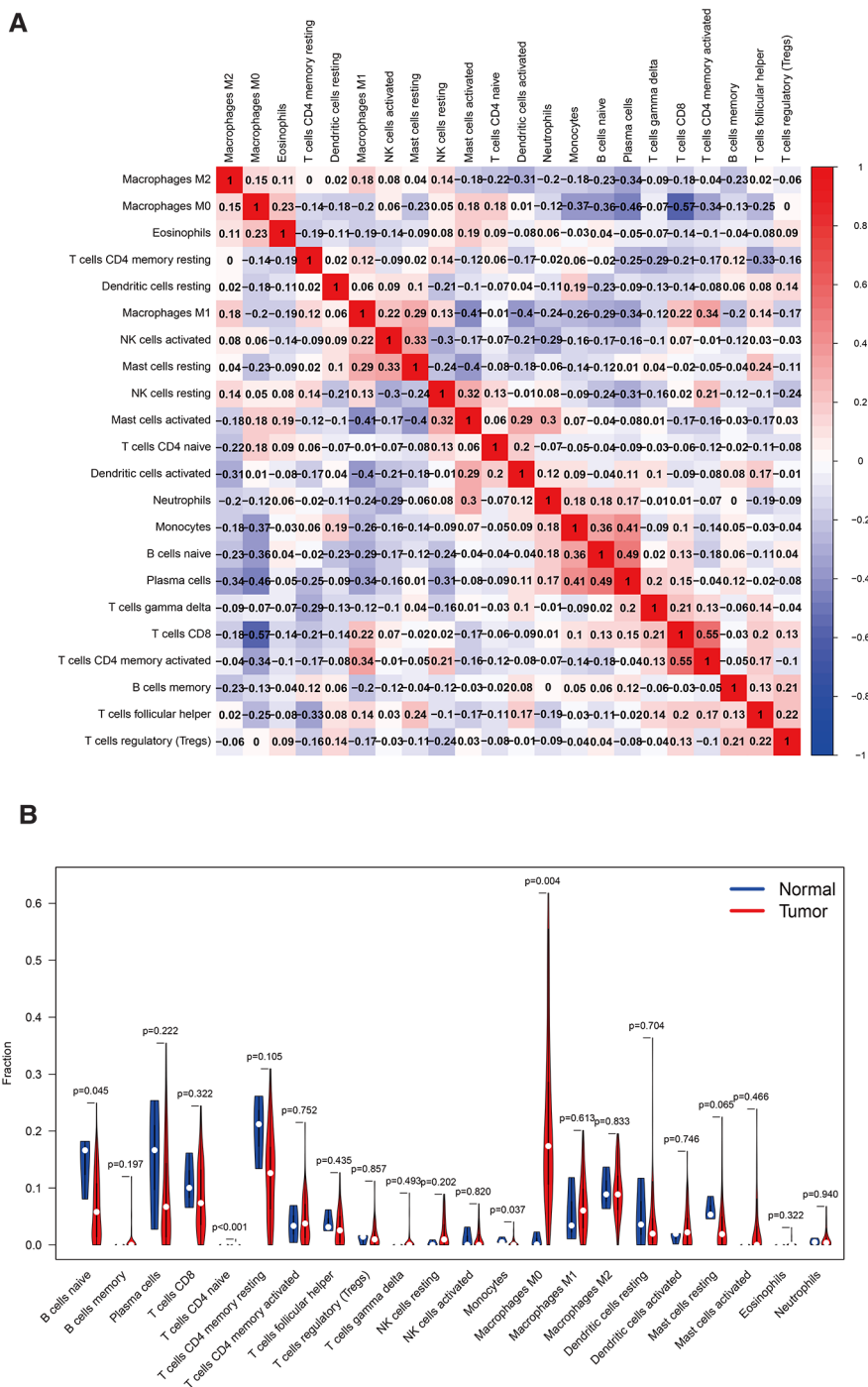


**Figure 7.** (A) Correlation heatmap of 22 immune cells. The color of the square represents the correlation between the 2 immune cells. (B) The expression difference of 22 immune cells in normal samples and patient samples. The blue violin column represents the normal sample, and the red violin column represents the patient sample. The p-value of the 2 sets of samples after the rank-sum test is located above the violin column.

the progression of several cancers. TMEM158 was significantly upregulated in pancreatic cancer samples. Studies of the mechanism have demonstrated that the activation of TGFβ1 and PI3K/AKT signals may be the aggressive cause of TMEM158 triggering pancreatic cancer. TGFβ1 has the effect of promoting carcinogenesis. A study demonstrated that TMEM158 was an upstream regulator of TGFβ1 by western blot, qRT-PCR, and ELISA experiments. Blockade of TGFβ1 significantly reversed TMEM158 overexpression-induced pancreatic cancer cell metastasis and epithelial-mesenchymal transition. PI3K/AKT signaling has been widely implicated in cancer cell proliferation,

metastasis, and apoptosis. TMEM158 was able to stimulate increased PI3K/AKT signaling in pancreatic cancer cells. Inhibiting the expression of TMEM158 can effectively reverse the pancreatic cancer cell proliferation, migration, and invasion induced by PI3K/AKT signaling.<sup>[54]</sup> SLC35C1 is a GDP fucose transporter negatively regulating the WNT signal pathway. In HEK293 cells, the silence of SLC35C1 can activate the WNT pathway, while the hyperexpression of SLC35C1 suppresses this pathway. WNT plays an important role in the maintenance of homeostasis, and abnormal activation of the WNT pathway is associated with a variety of cancers. SLC35C1 is a negative



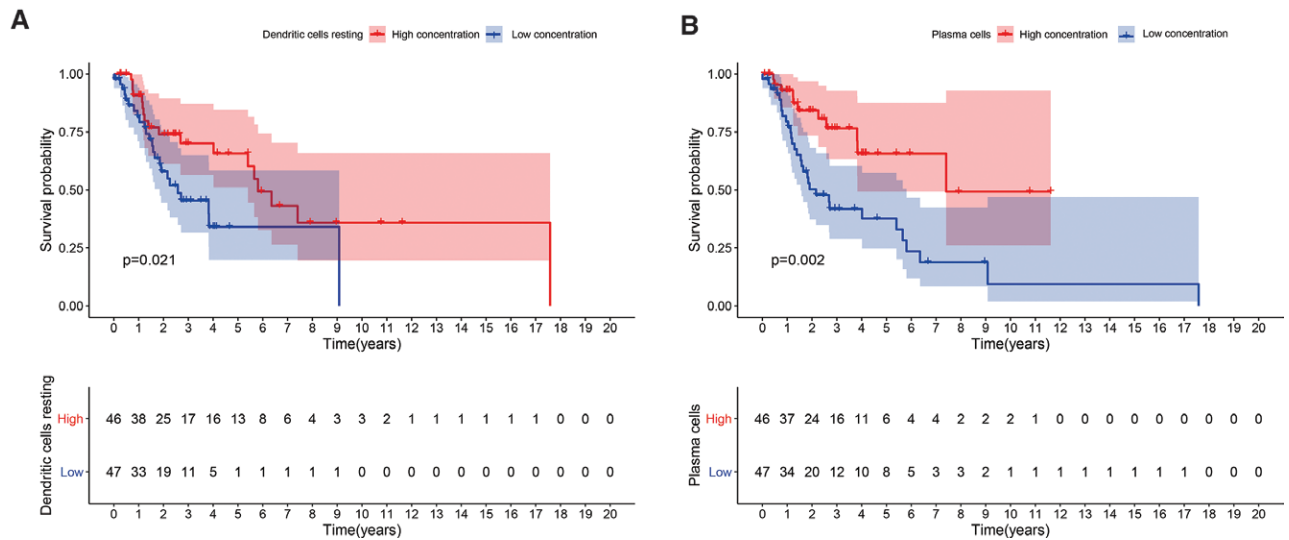


**Figure 8.** (A)The influence of Dendritic cells resting on the prognosis of patients with LSCC. (B)The influence of plasma cells on the prognosis of patients with LSCC.

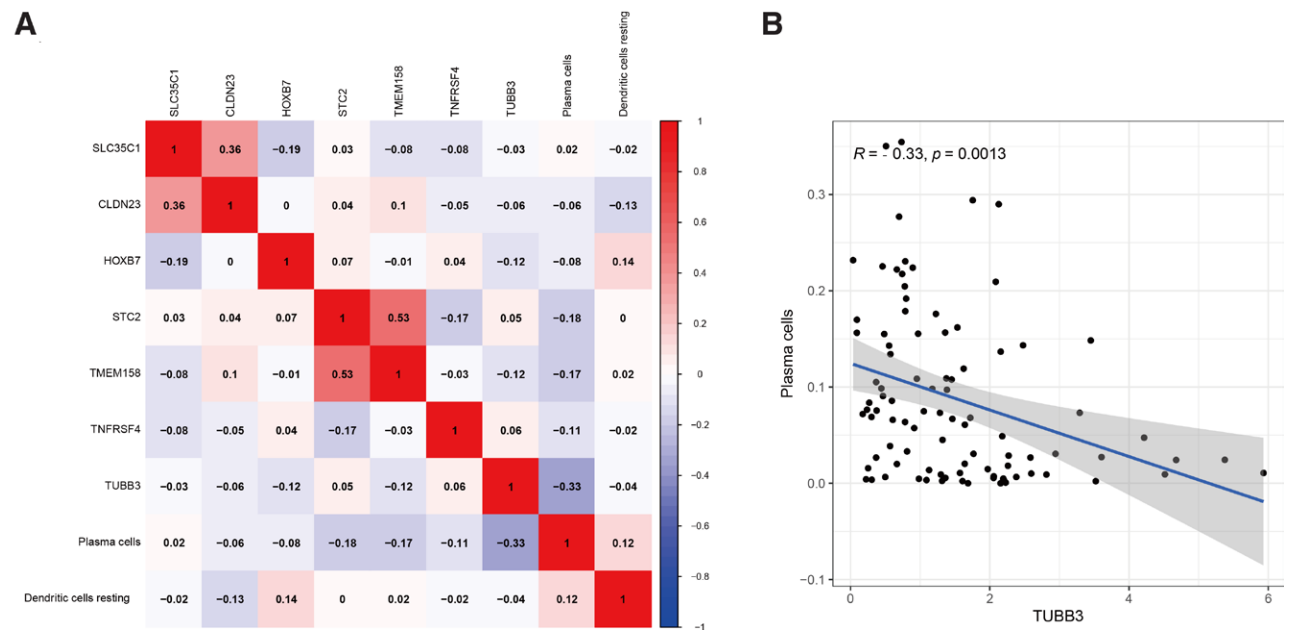


**Figure 9.** (A) Correlation analysis between key members of ceRNA network and key members of immune cells. (B) Scatter plot of the correlation between TUBB3 and plasma cells.

regulator for the WNT signaling pathway. Its abnormal expression may lead to over-activation of WNT signaling in cancer cells.<sup>[55]</sup> CLDN23 is the encoded gene of claudin-23. CLDN23 showed low expression in tumor patient samples in GEO and TCGA databases. The expression of CLDN23 is also downregulated in other types of tumors.<sup>[41]</sup> For example, intestinal tumors can reduce the expression of CLDN23. CLDN23 is reduced in tumor tissue compared to nearby normal mucosa.<sup>[56]</sup> However, survival analysis showed that low expression of CLDN23 was associated with longer OS. In previous studies, the relationship between CLDN23 and OS was controversial. Studies have reported that lower CLDN23 mRNA levels are associated with poorer OS.<sup>[40,57]</sup> There is also a Cox multivariate survival analysis showing that when CLDN23 is low expressed, the OS of gastric cancer patients is longer.<sup>[58]</sup> A recent study showed that low expression of CLDN23 was associated with longer OS in colorectal cancer patients of CMS4 and C4 subtypes. In contrast, in

the CMS2 and C1 subtypes, low CLDN23 expression was associated with shorter OS. It was shown that CLDN23 plays a dual role as a tumor suppressor/promoter in colorectal cancer.<sup>[59]</sup> Therefore, the effect of CLDN23 on prognosis is controversial, possibly because CLDN23 in different subtypes has different effects on prognosis, and our study did not divide the samples into subtypes. HOXB7 is the coding gene of homeobox protein Hox-B7. Previous studies have proved that HOXB7 activation may be a functional bridge between the homeobox gene and tumor progression. Besides, HOXB7 can also induce other genes to be directly or indirectly related to angiogenesis and tumor invasion. Vascular endothelial growth factors, interleukin-8, and angiopoietin-2 can all be upregulated by HOXB7 transduction.<sup>[60-62]</sup> In a study of patients with pancreatic cancer, HOXB7 mRNA and protein levels increased significantly in pancreatic ductal adenocarcinoma cell lines and patient tumor samples compared to normal samples. Tissue microarray evaluation of

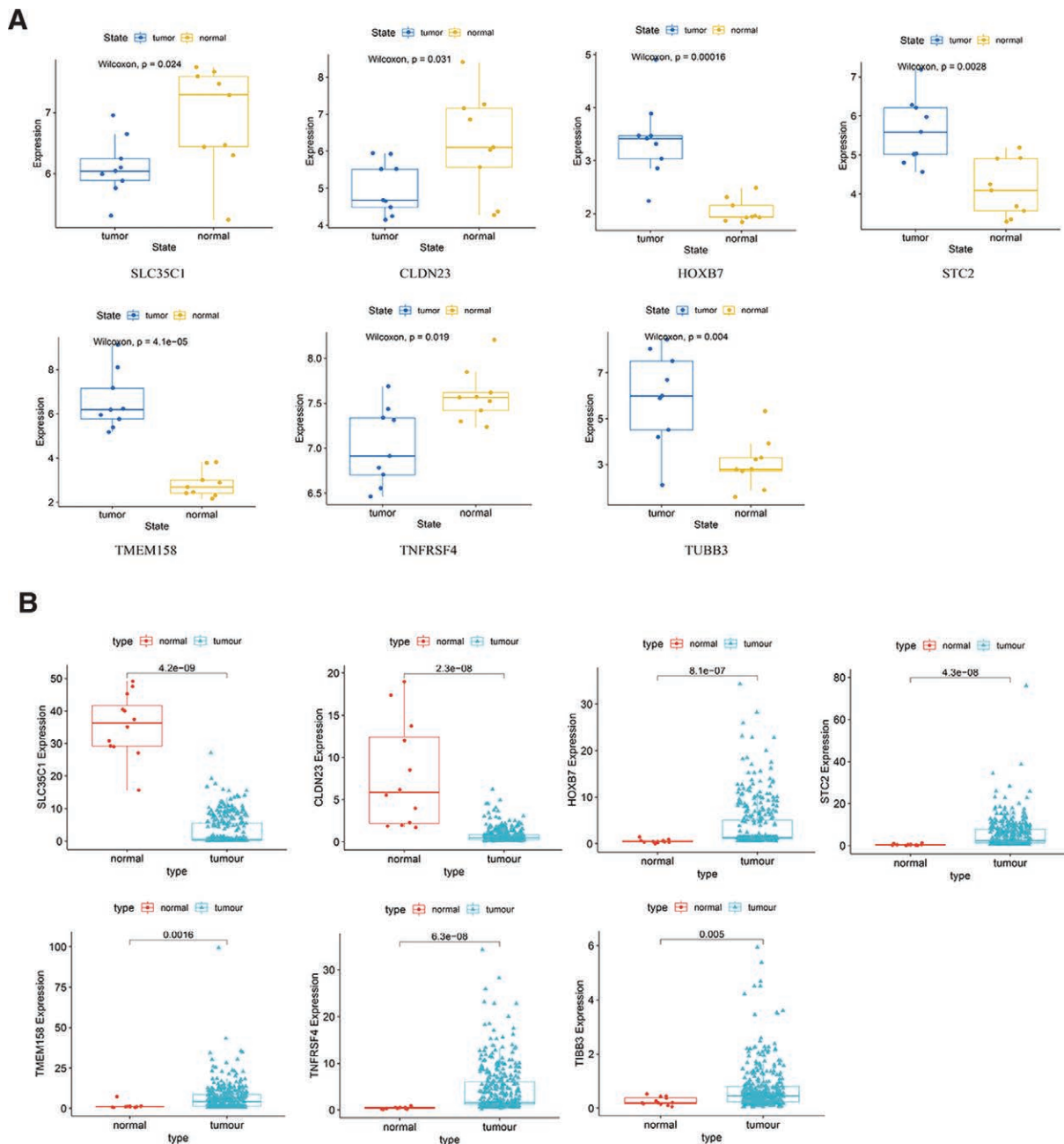


**Figure 10.** (A) Based on the GSE84957 data set, the expression of key mRNA in LSCC and normal samples was verified. The box plot shows mRNA expression in laryngeal carcinoma (blue) and corresponding normal tissues (yellow). (B) Based on the TCGA database, the expression of key mRNA in LSCC and normal samples was verified. The box plot shows mRNA expression in laryngeal carcinoma (blue) and corresponding normal tissues (red). The numbers in the table represent the number of studies included in the oncomine database. (C) Based on the oncomine database, identify the expression of key mRNA in different tumors. Red and blue represent upregulation or downregulation, respectively. (D) Based on the Kaplan–Meier database, the key mRNA in the model was validated for the prognosis of LSCC.

145 pancreatic ductal adenocarcinoma samples revealed that high expression of HOXB7 protein was associated with lymph node metastasis ( $P = .034$ ), which resulted in poor prognostication in patients. Knocking out or overexpression of HOXB7 in pancreatic ductal adenocarcinoma cell lines leads to decreased or increased invasiveness, respectively. HOXB7, together with its downstream targets may become new clinical biomarkers or therapeutic targets.<sup>[63]</sup> TUBB3 is the gene encoding the tubulin beta-3 chain. Overexpression of TUBB3 has been found to be related to the poor prognosis of some solid tumors including HNSCC. A study performed immunohistochemical staining on 667 cases of oral cancer, hypopharyngeal cancer, and LSCC tissues to detect the expression of TUBB3. It was demonstrated

that more than 90% of tumors showed clear cytoplasmic TUBB3 expression. 69 cases (15.5%) were weakly positive, 149 cases (33.5%) were moderately positive, and 188 cases (42.2%) were strongly positive.<sup>[64]</sup> Other studies have shown that some miRNAs, such as miR-200b-3p, can regulate the resistance of colorectal cancer cells to oxaliplatin by targeting TUBB3. It may be a potential drug target for colon cancer.<sup>[65]</sup> However, there are few studies on these genes in LSCC.

Dendritic cells are the most powerful professional antigen-presenting cells. Mature dendritic cells can effectively activate the initial T cells, at the center of initiating, regulating, and maintaining the immune response. A dendritic cell is closely related to the occurrence and development of tumors.

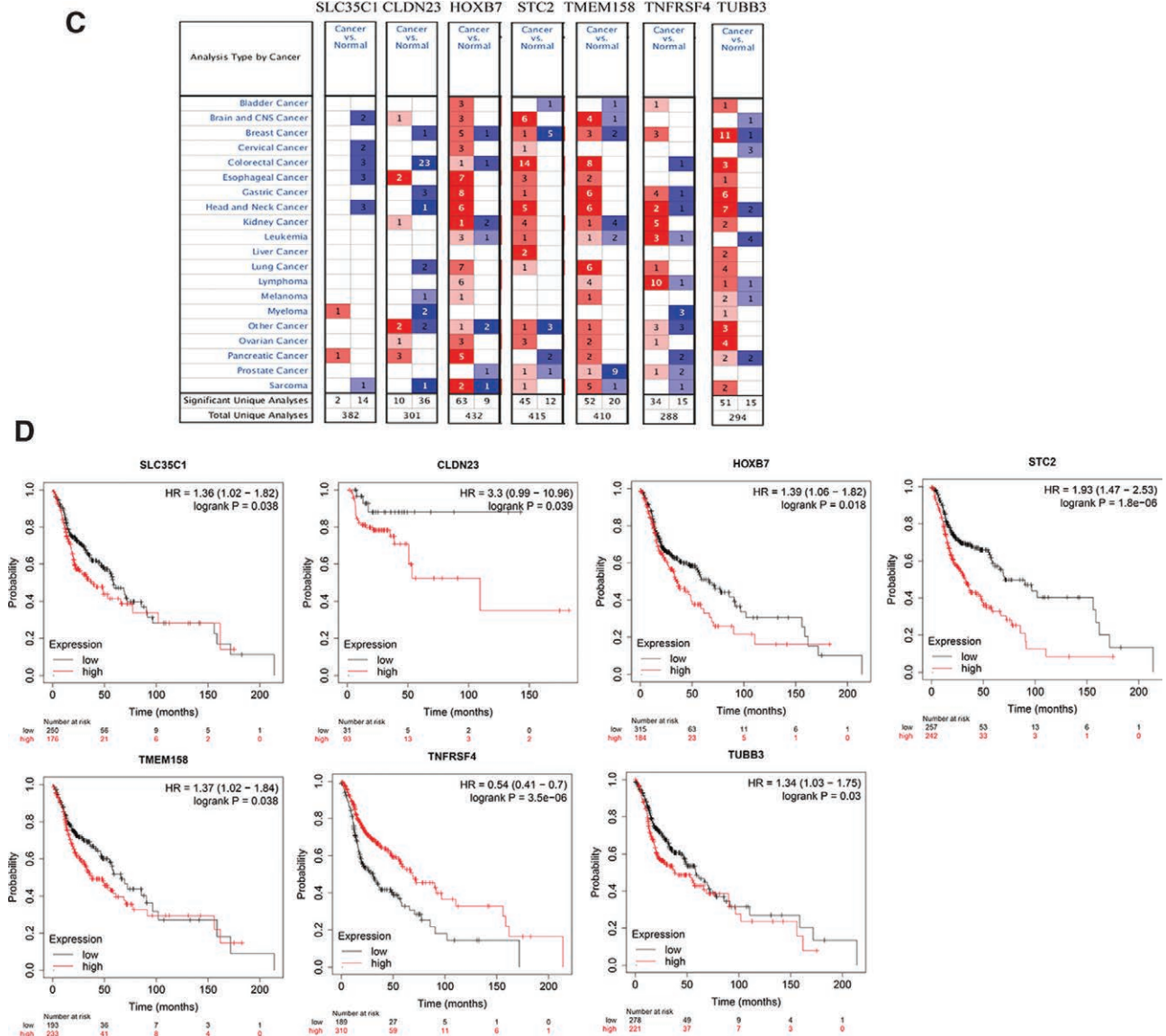


Figure 10. Continued

A large number of dendritic cells in most solid tumors results in a good prognosis. The cellular immune response dominated by CD8+ T cells is the basis of dendritic cells as an immunotherapy method.<sup>[66]</sup> Dendritic cells can induce high expression of major histocompatibility complex I and major histocompatibility complex II molecules. Major histocompatibility complex molecules bind to tumor antigens to form peptide-major histocompatibility complex molecular complexes. It is then presented to T cells to initiate the major histocompatibility complex I restricted cytotoxic T lymphocyte response and the major histocompatibility complex II-restricted CD4+ Th1 response.<sup>[67]</sup> At the same time, dendritic cells also provide the second signal required for T cell activation through costimulatory molecules (CD80/B7-1, CD86/B7-2, CD40, etc.) to initiate an immune response.<sup>[68]</sup> The combination of dendritic cells and T cells can secrete a large amount of IL-12 and IL-18 to activate T cell proliferation, which is conducive to tumor clearance. Dendritic cells can secrete chemotactic cytokines and upregulate the expression of IL-12, CD80, and CD86.<sup>[69]</sup> In addition, Dendritic cells also present antigen peptides directly to CD8+ T cells. CD4+ and CD8+ T cells can further enhance the anti-tumor immune response by secreting cytokines.

Plasma cells, also called effector B cells, are cells in the immune system that release large amounts of antibodies. It was indicated in a retrospective study that in 69 studies of 19 cancers, 50.0% of patients reported a positive effect of plasma cells on prognosis, while the rest had a neutral (40.7%) or negative (9.3%) effect. When plasma cells are present, the prognostic effect of T cells is generally stronger.<sup>[70]</sup> In addition, 21 studies inferred the proportion of plasma cells from gene expression data, most of which presented positive predictive effects. There is plenty of evidence to support the positive role of plasma cells in anti-tumor immunity.<sup>[71]</sup> Our results indicate that high concentrations of dendritic cells and plasma cells are associated with a better prognosis. This is consistent with previous reports in the literature.

In the correlation analysis, a significant positive correlation was found between SLC35C1 and CLDN23, STC2 and TMEM158, and a significant negative correlation between TUBB3 and plasma cells. From our research, a high level of plasma cells can make patients have a better prognosis. In tumor tissues, TUBB3 was significantly higher than that in adjacent tissues, while patients with high levels of TUBB3 were at higher risk. The results of the final analysis are consistent with the results of these studies. Plasma cell and TUBB3 ( $R = -0.33$ ,

$P = .0013$ ) showed a significant negative correlation. Therefore, we reasoned that plasma cells and TUBB3 may play critical roles in the progression of LSCC. However, after a systematic literature review, there are no relevant biological experiments to support our computational results. We will continue to explore the underlying mechanisms by which plasma cells and TUBB3 affect LSCC in future work.

Inevitably, some related limitations and shortcomings must be acknowledged. First of all, the amount of data collected from public databases is limited, in that the clinical samples analyzed in our research are relatively incomplete. At present, despite the rapid development of omics technology, a large number of research projects on detecting activity indicators are already feasible.<sup>[72]</sup> Large-scale experimental data is still difficult to obtain with very expensive testing costs as well.<sup>[73]</sup> Last but not least, the biggest problem in this study is the lack of validation of key genetic mechanisms. However, in order to reduce this bias, we also used multiple databases to reveal the gene expression of key biomarkers in tumors and adjacent tissues.

## 5. Conclusion

As for differentially expressed mRNAs and lncRNAs, a ceRNA prognostic risk model was constructed to predict survival and prognosticity in patients with LSCC. The higher AUC value proves the accuracy of our model. We have identified HOXB7, STC2, TMEM158, TUBB3, and other key genes related to the prognosis from the ceRNA network. Immune microenvironment analysis found that high levels of Dendritic cells and plasma cells will give patients a better prognosis. The co-expression analysis also illustrated that plasma cells and TUBB3 are related, which suggested that they may jointly affect the prognosis of LSCC patients.

## Acknowledgments

The authors gratefully acknowledge the support of this work by the Scientific Research Fund Project of the Hebei Provincial Health Commission (No. 20201146).

## Reference

- [1] Yue PJ, Sun YY, Li YH, et al. MYCT1 inhibits the EMT and migration of laryngeal cancer cells via the SP1/miR-629-3p/ESRP2 pathway. *Cell Signal*. 2020;74:109709109709.
- [2] Wu WK, Guo JL. Multifunctional zinc metal-organic framework for highly selective detection of picric acid and inhibition of laryngeal cancer cell growth. *J Cluster Sci*. 2020;31:435–43.
- [3] Zhang G, Fan E, Yue G, et al. Five genes as a novel signature for predicting the prognosis of patients with laryngeal cancer. *J Cell Biochem*. 2020.
- [4] Beck AJCC, Harten WHV, Brekel MWMVD, et al. Cost-effectiveness of surgery versus organ preservation in advanced laryngeal cancer: CEA laryngectomy vs. organ preservation. *Laryngoscope* 2020.
- [5] Faisal M, Malik KI, Hussain R, et al. Jamshed A: Incidence of thyroid gland invasion in advanced laryngeal cancers and its impact on disease-specific survival; a retrospective review at a tertiary care center. *Acta Otolaryngol*. 2020.
- [6] Nittala M, Mundra E, Smith M, et al. Vijayakumar s: improved clinical outcomes with shorter intervals between surgery and postoperative radiotherapy in t4 laryngeal cancers. *Int J Radiat Oncol Biol Phys*. 2020;108:E40.
- [7] Tong R, Zhang JR, Wang CY, et al. LncRNA PTCSC3 inhibits the proliferation, invasion and migration of cervical cancer cells via sponging miR-574-5p. *Clin Exp Pharmacol Physiol*. 2020;47:439–48.
- [8] Wang ZY, Liu TY, Li GQ, et al. The exploration of new therapeutic targets for HPV-negative head and neck squamous cell cancer through the construction of a ceRNA network and immune microenvironment analysis. *J Cell Biochem*. 2020;121:3426–37.
- [9] Wang LJ, Wang H, Xu K, et al. Exploration of immune-related cells and ceRNA in squamous cell lung cancer. *Med* 2021;100.

- [10] Luo Y, Li HJ, Huang HL, et al. Integrated analysis of ceRNA network in hepatocellular carcinoma using bioinformatics analysis. *Med* 2021;100.
- [11] Decmann A, Perge P, Turai PI, et al. Non-coding RNAs in adrenocortical cancer: from pathogenesis to diagnosis. *Cancers* 2020;12:461.
- [12] Ye YF, Shen A, Liu AW. Long non-coding RNA H19 and cancer: a competing endogenous RNA. *Bull Cancer*. 2019;106:1152–9.
- [13] Sassenberg M, Droop J, Schulz WA, et al. Upregulation of the long non-coding RNA CASC9 as a biomarker for squamous cell carcinoma. *Bmc Cancer* 2019;19.
- [14] Thomson DW, Dinger ME. Endogenous microRNA sponges: evidence and controversy. *Nat Rev Genet*. 2016;17:272–83.
- [15] Ginefra P, Lorusso G, Vannini N. Innate immune cells and their contribution to t-cell-based immunotherapy. *Int J Mol Sci*. 2020;21:4441.
- [16] Wei FQ, Sun W, Wong TS, et al. Eliciting cytotoxic T lymphocytes against human laryngeal cancer-derived antigens: evaluation of dendritic cells pulsed with a heat-treated tumor lysate and other antigen-loading strategies for dendritic-cell-based vaccination. *J Exp Clin Cancer Res* 2016;35.
- [17] Wang F, Zhou L, Chen N, et al. The effect of pretreatment BMI on the prognosis and serum immune cells in advanced LSCC patients who received ICI therapy. *Medicine* 2021;100:e24664.
- [18] Zeng H, Huang YQ, Chen LY, et al. Exploration and validation of the effects of robust co-expressed immun-related genes on immune infiltration patterns and prognosis in laryngeal cancer. *Int Immunopharmacol*. 2020;85.
- [19] Newman AM, Steen CB, Liu CL, et al. Determining cell type abundance and expression from bulk tissues with digital cytometry. *Nat Biotechnol*. 2019;37:773–82.
- [20] Newman AM, Liu CL, Green MR, et al. Robust enumeration of cell subsets from tissue expression profiles. *Nat Methods*. ;12:453
- [21] Ali HR, Chlon L, Pharoah PDP, et al. Patterns of immune infiltration in breast cancer and their clinical implications: a gene-expression-based retrospective study. *PLoS Med*. 2016;13:e1002194.
- [22] Liu XY, Wu SC, Yang YH, et al. The prognostic landscape of tumor-infiltrating immune cell and immunomodulators in lung cancer. *Biomed Pharmacother*. 2017;95:55–61.
- [23] Zhou LY, Li YJ, Wei G, et al. Assessment of tumor-associated immune cells in laryngeal squamous cell carcinoma. *J Cancer Res Clin Oncol*. 2019;145:1761–72.
- [24] Kong XR, Qi JX, Yan Y, et al. Comprehensive analysis of differentially expressed profiles of lncRNAs, mRNAs, and miRNAs in laryngeal squamous cell carcinoma in order to construct a ceRNA network and identify potential biomarkers. *J Cell Biochem*. 2019;120:17963–74.
- [25] Deng M, Gelmann J, Schultze JL, et al. Web-TCGA: an online platform for integrated analysis of molecular cancer data sets. *BMC Bioinf*. 2016;17:72.
- [26] Zhang Y, Wagner EK, Guo X, et al. Long intergenic non-coding RNA expression signature in human breast cancer. *Sci Rep*. 2016;6:37821.
- [27] Robinson MD, McCarthy DJ, Smyth GK. edgeR: a Bioconductor package for differential expression analysis of digital gene expression data. *Bioinformatics* 2009;1.
- [28] Ashwini Jeggarisup/sup DSMs, Erik Larssonsup/sup: miRcode: a map of putative microRNA target sites in the long non-coding transcriptome. *Bioinform*. 2012;28:2062–3.
- [29] Chen Y, Wang X. miRDB: an online database for prediction of functional microRNA targets. *Nucl Acids Research*. 2019:D1.
- [30] Chou CH, Shrestha S, Yang CD, et al. miRTarBase update 2018: a resource for experimentally validated microRNA-target interactions. *Nucleic Acids Res*. 2018;46:D296–302.
- [31] Shi Y, Yang F, Wei S, et al. Identification of key genes affecting results of hyperthermia in osteosarcoma based on integrative ChIP-seq/targetscan Analysis. *Med Sci Monit*. 2017;23:2042–8.
- [32] Barrett T, Troup DB, Wilhite SE, et al. NCBI GEO: archive for functional genomics data sets - update. *Nucleic Acids Res*. 2011;39:D1005–1010.
- [33] Feng L, Wang R, Lian M, et al. Integrated analysis of long noncoding RNA and mRNA expression profile in advanced laryngeal squamous cell carcinoma. *PLoS One*. 2016;11.
- [34] Xi R, Evans J, Chae H, et al. Abstract 5013: CpG island shore methylation regulates caveolin-1 expression in breast cancer. *Cancer Res*. 2012;72(8 Supplement):5013–5013.
- [35] ONCOMINE. A cancer microarray database and integrated data-mining platform. *Neoplasia* 2004;6:1–6.
- [36] Qi ZT, Liu YT, Mints M, et al. Single-cell deconvolution of head and neck squamous cell carcinoma. *Cancers* 2021;13.

- [37] Zhang Y, Chen P, Zhou Q, et al. A novel immune-related prognostic signature in head and neck squamous cell carcinoma. *Front Genet.* 2021;12.
- [38] Huang C, He J, Dong Y, et al. Identification of novel prognostic markers associated with laryngeal squamous cell carcinoma using comprehensive analysis. *Front Oncol.* 2022;11.
- [39] Deng MZ, Chen ZH, Tan JQ, et al. Down-regulation of SLC35C1 induces colon cancer through over-activating WNT pathway. *J Cell Mol Med.* 2020;24:3079–90.
- [40] Pitule P, Vycital O, Bruha J, et al. Differential expression and prognostic role of selected genes in colorectal cancer patients. *Anticancer Res.* 2013;33:4855–65.
- [41] Katoh M. Epithelial-mesenchymal transition in gastric cancer (Review). *Int J Oncol.* 2005;27:1677–83.
- [42] Singh A, Mohanty I, Singh J, et al. BDNF augments rat internal anal sphincter smooth muscle tone via RhoA/ROCK signaling and non-adrenergic noncholinergic relaxation via increased NO release. *Am J Physiol Gastrointest Liver Physiol.* ;318:G23–33.
- [43] Paco A, Leita-Castro J, et al. Epigenetic regulation of CDH1 is altered after HOXB7-silencing in MDA-MB-468 triple-negative breast cancer cells. *Genes* 2021;12.
- [44] Chen Y, Zhao XH, Zhang DD, et al. MiR-513a-3p inhibits EMT mediated by HOXB7 and promotes sensitivity to cisplatin in ovarian cancer cells. *Eur Rev Med Pharmacol Sci.* 2020;24:10391–402.
- [45] Ge LH, Peng SD, Tan H, et al. Inhibition of HOXB7 gene expression in melanoma cells by small interfering RNA. *Chinese Journal of Cancer Research.* 2008;20:90–9.
- [46] Liu ZZ, Liu ZT, Zhou X, et al. A glycolysis-related two-gene risk model that can effectively predict the prognosis of patients with rectal cancer. *Hum Genomics.* 2022;16.
- [47] Zhang CX, Chen SQ, Ma X, et al. Upregulation of STC2 in colorectal cancer and its clinicopathological significance. *Oncotarget Therapy* 2019;12:1249–58.
- [48] Li JB, Wang XY, Chen LL, et al. TMEM158 promotes the proliferation and migration of glioma cells via STAT3 signaling in glioblastomas. *Cancer Gene Ther.*
- [49] Song FC, Yang Y, Liu JX. MicroRNA-548ac induces apoptosis in laryngeal squamous cell carcinoma cells by targeting transmembrane protein 158. *Oncol Lett.* 2020;20.
- [50] Liu LH, Zhang JT, Li SQ, et al. Silencing of TMEM158 inhibits tumorigenesis and multidrug resistance in colorectal cancer. *Nutr Cancer.* 2020;72:662–71.
- [51] Li MY, Cao W, Huang BQ, et al. Establishment and analysis of an individualized immune-related gene signature for the prognosis of gastric cancer. *Frontiers in Surgery* 2022;9.
- [52] Yi M. TUBB3 promotes growth and invasion of gallbladder cancer cells by Akt/mTOR signal pathway. *J Environ Pathol Toxicol Oncol.* 2021;40.
- [53] Jia YJ, Sung SL, Gao X, et al. Expression levels of TUBB3, ERCC1 and P-gp in ovarian cancer tissues and adjacent normal tissues and their clinical significance. *J Buon.* 2018;23:1390–5.
- [54] Fu Y, Yao N, Ding D, et al. TMEM158 promotes pancreatic cancer aggressiveness by activation of TGFβ1 and PI3K/AKT signaling pathway. *J Cell Physiol.* 2020;11.
- [55] Deng M, Chen Z, Tan J, et al. Down regulation of SLC35C1 induces colon cancer through over-activating Wnt pathway. *J Cell Mol Med.* 2020;24.
- [56] Katoh M, Katoh M. MCLDN23 gene, frequently down-regulated in intestinal-type gastric cancer, is a novel member of CLAUDIN gene family. *Int J Mol Med.* 2003;11:683–9.
- [57] Yang LQ, Zhang WQ, Li M, et al. Evaluation of the prognostic relevance of differential claudin gene expression highlights claudin-4 as being suppressed by TGF beta 1 inhibitor in colorectal cancer. *Front Genet.* 2022;13.
- [58] Lu YZ, Jing JJ, Sun LP, et al. Expression of claudin-11,-23 in different gastric tissues and its relationship with the risk and prognosis of gastric cancer. *PLoS One.* 2017;12.
- [59] Cherradi S, Martineau P, Gongora C, et al. Claudin gene expression profiles and clinical value in colorectal tumors classified according to their molecular subtype. *Cancer Manag Res.* 2019;11:1337–48.
- [60] How C, Hui ABY, Alajez NM, et al. MicroRNA-196b regulates the homeobox b7-vascular endothelial growth factor axis in cervical cancer. *PLoS One.* 2013;8.
- [61] Dai LF, Hu WD, Yang ZJ, et al. Upregulated expression of HOXB7 in intrahepatic cholangiocarcinoma is associated with tumor cell metastasis and poor prognosis. *Lab Invest.* 2019;99:736–48.
- [62] Meccia E. HOXB7: a key factor for tumor-associated angiogenic switch. *Cancer Res.* 2001;61:6532–9.
- [63] Kovoichich AN, Arensman M, Lay AR, et al. HOXB7 promotes invasion and predicts survival in pancreatic adenocarcinoma. *Cancer* 2013;119.
- [64] Nienstedt JC, Grbe A, Clauditz T, et al. High level βIII tubulin overexpression occurs in most head and neck cancers but is unrelated to clinical outcome. *J Oral Pathology Med.* 2017.
- [65] Wu YZ, Lin HY, Zhang Y, et al. miR-200b-3p mitigates oxaliplatin resistance via targeting TUBB3 in colorectal cancer. *J Gene Med.* 2020;22.
- [66] Sato T, Terai M, Yasuda R, et al. Combination of monocyte-derived dendritic cells and activated T cells which express CD40 ligand: a new approach to cancer immunotherapy. *Cancer Immunol Immunother.* 2004;53:53–61.
- [67] Wang YY, Liu HZ, Cao M, et al. Mechanism of miRNA-based Aconitum leucostomum Worosch. Monomer inhibition of bone marrow-derived dendritic cell maturation. *Int Immunopharmacol.* 2020;88:106791.
- [68] Akhtar N, Mishra M, Yadav V, et al. Runx proteins mediate protective immunity against Leishmania donovani infection by promoting CD40 expression on dendritic cells. *PLoS Pathog.* 2020;16:e1009136.
- [69] Alvarez D, Vollmann EH, Andrian UHV. Mechanisms and consequences of dendritic cell migration. *Immunity* 2008;29:325–42.
- [70] Grigoriadis G, Gilbertson M, Came N, et al. Is CD20 positive plasma cell myeloma a unique clinicopathological entity? A study of 40 cases and review of the literature. *Pathology* 2012;44:552.
- [71] Maartje C, Wouters BN. Prognostic significance of tumor-infiltrating B cells and plasma cells in human cancer. *Clin Cancer Res Official J Am Assoc Cancer Res.* 2018.
- [72] Liu J, Lichtenberg T, Hoadley KA, et al. An integrated TCGA pan-cancer clinical data resource to drive high-quality survival outcome analytics. *Cell.* 2018.
- [73] Huo M, Zhang Y, Chen Z, et al. Tumor microenvironment characterization in head and neck cancer identifies prognostic and immunotherapeutically relevant gene signatures. *Sci Rep.* 2020;10:11163.